THE JOURNAL OF BIOLOGICAL CHEMISTRY VOL. 286, NO. 16, pp. 14110–14119, April 22, 2011

Protein Kinase A Is Central for Forward Transport of Two-pore Domain Potassium Channels $K_{2P}3.1$ and $K_{2P}9.1$*[S]

Received for publication, October 1, 2010, and in revised form, February 6, 2011 Published, JBC Papers in Press, February 28, 2011, DOI 10.1074/jbc.M110.190702

Alexandra Mant[‡], David Elliott[§], Patrick A. Eyers[¶], and Ita M. O'Kelly[‡1]

From the [‡]Division of Human Genetics, Centre for Human Development, Stem Cells and Regeneration, University of Southampton, Duthie Building, Mail Point 808, Southampton General Hospital, Tremona Road, Southampton SO16 6YD, United Kingdom, the [§]Institute of Molecular and Cellular Biology, University of Leeds, Leeds LS2 9JT, United Kingdom, and the [¶]Yorkshire Cancer Research, Institute for Cancer Studies, University of Sheffield, Sheffield S10 2RX, United Kingdom

Acid-sensitive two-pore domain potassium channels ($K_{2P}3.1$ and $K_{2P}9.1$) play key roles in both physiological and pathophysiological mechanisms, the most fundamental of which is control of resting membrane potential of cells in which they are expressed. These background "leak" channels are constitutively active once expressed at the plasma membrane, and hence tight control of their targeting and surface expression is fundamental to the regulation of K^+ flux and cell excitability. The chaperone protein, 14-3-3, binds to a critical phosphorylated serine in the channel C termini of $K_{2P}3.1$ and $K_{2P}9.1$ (Ser^{393} and Ser^{373}, respectively) and overcomes retention in the endoplasmic reticulum by βCOP. We sought to identify the kinase responsible for phosphorylation of the terminal serine in human and rat variants of $K_{2P}3.1$ and $K_{2P}9.1$. Adopting a bioinformatic approach, three candidate protein kinases were identified: cAMP-dependent protein kinase, ribosomal S6 kinase, and protein kinase C. *In vitro* phosphorylation assays were utilized to determine the ability of the candidate kinases to phosphorylate the channel C termini. Electrophysiological measurements of human $K_{2P}3.1$ transiently expressed in HEK293 cells and cell surface assays of GFP-tagged $K_{2P}3.1$ and $K_{2P}9.1$ enabled the determination of the functional implications of phosphorylation by specific kinases. All of our findings support the conclusion that cAMP-dependent protein kinase is responsible for the phosphorylation of the terminal serine in both $K_{2P}3.1$ and $K_{2P}9.1$.

Two-pore domain (K_{2P}) potassium channels are widely expressed and play a vital role in stabilizing cellular membrane potential. The acid-sensitive K_{2P} subgroup (TASK) $K_{2P}3.1$ (also known as TASK1) and $K_{2P}9.1$ (TASK3) are inactivated by low external pH (1). TASK channels are implicated in playing regulatory roles in cell proliferation (and oncogenesis), chemoreception, activation of T-cells, and have neuroprotective roles in response to ischemia and inflammation (1). These channels are sensitive to an array of physiological and pharmacological modulators, including extracellular acidification, hypoxia, local anesthetics, and endocannabinoids (2–10). K_{2P} channels are constitutively active once expressed on the cell surface and therefore "leak" potassium from the cell via highly regulated pathways. Consequently, these channels are key contributors to the resting membrane potential of cells and are therefore vital components in determining the characteristics of cell excitability. The control of channel surface expression and targeting to the cell membrane are of critical importance because any change in the channel number at the plasma membrane influences the electrical properties of the cell in which they are expressed. K_{2P} channel activity is regulated via quality control pathways, which control the targeting, cell surface delivery, and recovery of these channels.

We and others have demonstrated that the export of newly synthesized $K_{2P}3.1$ channels from the endoplasmic reticulum to the cell surface is subject to tight quality control mechanisms (11–15). Although the exact roles and binding domains of regulators are disputed, there is general agreement that regulation of forward transport of $K_{2P}3.1$ and $K_{2P}9.1$ is dependent on their interaction with either 14-3-3, a ubiquitously expressed chaperone protein, or βCOP, a component of the multiprotein coatomer-coated vesicle COPI. Dibasic endoplasmic reticulum retrieval motifs bind βCOP and inhibit forward transport of the channel to the membrane, whereas recruitment of 14-3-3 to a non-canonical 14-3-3 binding motif (MKRRSSV-cooh) at the channel C terminus overcomes βCOP binding and enables forward transport of the channels to the membrane (11, 12, 14). We previously observed 14-3-3 recruitment to the $K_{2P}3.1$ C terminus to be dependent on the phosphorylation of the penultimate C-terminal residue (-RRSpSV, where pS denotes phosphorylated serine). Disruption of this C-terminal motif eliminated 14-3-3β binding to the channel and trafficking of the channel to the plasma membrane. Replacing the terminal five residues with a canonical 14-3-3 motif, as found in Raf1 kinase (-RSApSEP), restored both 14-3-3β binding and cell surface expression (11).

14-3-3 proteins are an abundant, highly conserved family of ubiquitously expressed adaptor proteins that modulate a multitude of functionally diverse proteins, including functional expression of an expanding number of ion channels (16, 17). 14-3-3 binds to phosphoserine-containing motifs in a sequence-specific manner; our previous studies have shown that, although there are two potential phosphorylation sites within the C terminus of human $K_{2P}3.1$, 14-3-3 binding is dependent on phosphorylation of the terminal serine, Ser^{393} (11, 12, 14). A hitherto undetermined kinase is responsible for this phosphorylation. Here we investigate the phosphorylation

* This work was funded by Biotechnology and Biological Sciences Research Council Award BB/E014453/2 (to I. M. O.).
[S] The on-line version of this article (available at http://www.jbc.org) contains supplemental Figs. 1–4.
[1] To whom correspondence should be addressed. Tel.: 44-23-8079-6421; Fax: 44-23-8079-4264; E-mail: I.M.O'Kelly@southampton.ac.uk.

TABLE 1

$K_{2P}3.1$ and $K_{2P}9.1$ wild type and mutant C terminus sequences used in this study

Amino acid substitutions are shown in boldface type.

Channel	Experimental system	Sequence of C terminus	Mutation
$K_{2P}3.1$ human	Electrophysiology (full-length); *in vitro* kinase assays (C terminus fused to GST)	SLSTFRGLMKRRSSV	Wild type
		SLSTFRGLMKRRS**A**V	S393A
		SLSTFRGLMKRR**A**SV	S392A
		SLSTFRGLMKRR**AA**V	S392A/S393A
		SLSTFRGLMKRRS**D**V	S393D
		SLSTFRGLMKRRSS.	ΔV394
GFP-$K_{2P}3.1$-HA rat	Immunofluorescence; flow cytometry	SLATFRGLMKRRSSV	Wild type (Ala^{213}-HA-Leu^{214})
$K_{2P}9.1$ human	Electrophysiology (full-length); *in vitro* kinase assays (C terminus fused to GST)	SFTDHQRLMKRRKSV	Wild type
		SFTDHQRLMKRRK**A**V	S373A
$K_{2P}9.1$ rat	*In vitro* kinase assays (C terminus fused to GST)	TCGENHRLHIRRKSI	Wild type
		TCGENHRLHIRRK**A**I	S395A
GFP-$K_{2P}9.1$-His rat	Flow cytometry	SLATFRGLMKRRSSV	Wild type (Ala^{213}-His_6-Leu^{214})

of the human (h) and rat (r) $K_{2P}3.1$ and $K_{2P}9.1$ channels and present *in vitro* and *in vivo* evidence to demonstrate that the cAMP-dependent protein kinase (protein kinase A; PKA)[2] is responsible for phosphorylation of the terminal serine of $K_{2P}3.1$ and $K_{2P}9.1$, thus enabling forward transport of these channels.

EXPERIMENTAL PROCEDURES

Molecular Biology—Table 1 summarizes the constructs used and shows the sequence of the C-terminal 15 amino acids of each. WT $hK_{2P}3.1$ DNA in the vector pRAT was produced as described previously (11). Mutations to create alanine or aspartate substitutions in the C terminus of the full-length channel were made with an XL QuikChange kit (Stratagene, La Jolla, CA) and confirmed by DNA sequencing. HA-(YPYDVPDYA)-tagged $rK_{2P}3.1$ was created by QuikChange PCR mutagenesis of full-length $rK_{2P}3.1$ fused to N-terminal eGFP (a gift from Dr. R. Preisig-Müller, Philipps Universität, Marburg, Germany) in pcDNA3.1 (Invitrogen). The tag was introduced to an external loop of the second pore-forming domain, between alanine 213 and leucine 214. Similarly, a His (HHHHHH) tag was introduced into GFP-$rK_{2P}9.1$ between Ala^{213} and Leu^{214}.

The glutathione *S*-transferase (GST)-conjugated C terminus of $hK_{2P}3.1$ was created by annealing phosphorylated oligonucleotides encoding the final 15 amino acids of WT $hK_{2P}3.1$ (5′-AAT TCC ACA GTT TAT CGA CAT TTC GAG GTC TCA TGA AGC GAA GAA GCT CAG TGT AAT CGA GC-3′ and 5′-GGC CGC TCG ATT ACA CTG AGC TTC TTC GCT TCA TGA GAC CTC GAA ATG TCG ATA AAC TGT GG-3′) and ligating them into the pGEX-6P-1 plasmid (GE Healthcare) between the EcoRI and NotI sites in the multiple cloning site. Corresponding $hK_{2P}9.1$ and $rK_{2P}9.1$ constructs were made in a similar manner ($hK_{2P}9.1$, 5′-AAT TCA GCT TTA CCG ACC ACC AGA GGC TGA TGA AAC GCC GGA AGT CCG TTT AAA CCT CGA GC-3′ and 5′-GGC CGC TCG AGG TTT AAA CGG ACT TCC GGC GTT TCA TCA GCC TCT GGT GGT CGG TAA AGC TG-3′; $rK_{2P}9.1$, 5′-AAT TCA CCT GCG GGG AAA ACC ACA GGC TGC ACA TCC GTC GCA AGT CCA TTT AAA CCT CGA GC-3′ and 5′-GGC CGC TCG AGG TTT AAA TGG ACT TGC GAC GGA TGT GCA GCC TGT GGT TTT CCC CGC AGG TG-3′). Mutations were introduced by PCR, using the Stratagene QuikChange kit (Agilent Technologies UK Ltd., Stockport, UK), and all cDNAs and mutants were confirmed by DNA sequencing.

Recombinant Fusion Protein Expression—Cultures of *Escherichia coli* strain BL21 (DE3), containing constructs of $hK_{2P}3.1$ and $hK_{2P}9.1$ C termini fused to GST or GST alone, were grown at 37 °C, 200 rpm in 100 ml of LB medium plus 100 μg/ml ampicillin to OD 0.5 and then induced with 0.5 mM IPTG for 3 h. Bacteria were harvested by centrifugation and resuspended in 2 ml of PBS, 1 mM EDTA containing 2× Complete Protease Inhibitor Mixture (Roche Applied Science). Triton X-100 was added to 1% (v/v). Bacterial suspensions were sonicated in an ice water bath by a Misonix 3000 Sonicator (Misonix Inc., Farmingdale, NY) with cup horn probe for 3 × 1 min at power setting 1.5 and then centrifuged at 17,000 × *g* for 20 min at 4 °C. The supernatant was used as a substrate for *in vitro* phosphorylation assays.

In Vitro Phosphorylation Assays—The DNA sequence of the catalytic subunit of human PKA (PKAc) was amplified by PCR and cloned into the vector pET30 Ek/LIC (Novagen, Nottingham, UK). Recombinant His-tagged PKA was purified from the soluble supernatant of *E. coli* strain BL21(DE3) pLysS by IMAC, eluted in imidazole, and dialyzed into kinase buffer (50 mM Tris-HCl, pH 7.4, 150 mM NaCl, 0.1% 2-mercaptoethanol) prior to storage at −80 °C. Ribosomal protein S6 kinase 2 (RSK2), PKCα, MAPK I, and casein kinase II were purchased from Invitrogen. PKA assays contained 45 μl of sonicate supernatant (typically 160 μg of total protein), 1.5 μg of PKA, 50 mM Tris, pH 7.4, 100 mM NaCl, 0.1% 2-mercaptoethanol, 10 mM $MgCl_2$, and 100 μM ATP in a 180-μl total volume. RSK2 assays contained 45 μl of sonicate supernatant, 1.5 μg of RSK2, 50 mM Tris, pH 7.4, 10 mM $MgCl_2$, 2 mM DTT, 1 mM EGTA, 0.01% Triton X-100, and 100 μM ATP in a 180-μl total volume. PKC assays contained 45 μl of sonicate supernatant, 0.7 μg of PKCα, 50 mM Tris, pH 7.4, 100 mM NaCl, 0.1% 2-mercaptoethanol, 10 mM $MgCl_2$, 100 μM ATP, and 39 μl of lipid activator mix (Millipore, Watford, UK) in a 180-μl total volume. Samples were incubated for 30 min at 30 °C, and then the fusion proteins were purified using affinity resin. Glutathione-Sepharose was prepared according to the manufacturer's instructions (GE Healthcare) and 100 μl of slurry was added per sample. Tubes

[2] The abbreviations used are: PKA, protein kinase A; eGFP, enhanced green fluorescent protein; RSK, ribosomal protein S6 kinase; 8-Br-cAMP, 8-bromo-cyclic AMP.

were rotated end-on-end for 1 h at room temperature. Samples were centrifuged at 500 × *g* for 5 min at room temperature, and the Sepharose pellet was washed three times with 10 volumes of PBS, 1% (v/v) Triton X-100 and two times with 10 volumes of 50 mM Tris, pH 8.0. Fusion proteins were eluted twice from the resin, each time with 1 volume of 10 mM reduced glutathione, 50 mM Tris, pH 8.0, for 10 min at room temperature, and then the eluates were pooled and frozen at −20 °C. Positive control substrates for PKCα, MAPK, and casein kinase II were histone H1 and myelin basic protein (Millipore) and the casein kinase II substrate peptide RRRDDDSDDD fused to GST as described above.

Phos-tag Electrophoresis—Detection of phosphorylated proteins was achieved by SDS-PAGE incorporating Phos-tag acrylamide (Phos-tag Consortium, Hiroshima, Japan). 10% polyacrylamide gels (29:1 acrylamide/bisacrylamide) containing 50 μM Phos-tag ligand and 50 μM $MnCl_2$ were prepared according to the manufacturer's instructions. Eluted proteins were mixed with sample buffer, heated for 5 min at 95 °C, and electrophoresed at 30 mA/gel at room temperature. Gels were fixed and stained using InstantBlue (Expedeon, Cambridgeshire, UK).

Two-electrode Voltage Clamp Recordings—Oocytes were isolated from *Xenopus laevis* toads (Nasco, Atkinson, WI), treated with collagenase to ease removal of the follicular layer, and injected with 0.1–1 ng of $K_{2P}3.1$ WT or mutant channel cRNA in 46 nl of sterile water. Currents were measured 48 h after injection by two-electrode voltage clamp (Warner Instruments Corp., Hamden, CT). Data were filtered at 1 kHz and sampled at 4 kHz. Electrodes of 1.5-mm borosilicate glass tubes (Garner Glass Co., Claremount, CA) contained 3 M KCl and had resistances of 0.3–1 milliohm. Recordings were performed at room temperature with perfusion of 0.4–1.0 ml/min ND96 (93 mM NaCl, 5 mM KCl, 1 mM $MgCl_2$, 0.3 mM $CaCl_2$, 5 mM HEPES, pH 7.5 or 6.5, with NaOH or HCl). Holding potential was −80 mV. Currents were evoked by step depolarization from −135 to +60 mV in 15-mV increments. Acid sensitivity was routinely determined (data not shown) by exchanging external bath solutions during repeated step depolarization from holding potential to +30 mV at 10-s intervals.

Whole Cell Patch Clamping Recordings—HEK293 cells (10^5 cells/well) were plated on 22-mm sterile coverslips in 6-well plates in DMEM plus 10% FCS. Cells in each well were transiently transfected with 3.0 μg of untagged, full-length $hK_{2P}3.1$ in pRAT (11) and 1.5 μg of eGFP-C1 (Clontech), using jetPEI transfection reagent, according to the supplier's instructions (Polyplus, Source Bioscience Autogen, Nottingham, UK). Controls were either not incubated with transfection reagent or were transfected with 1.5 μg of eGFP-C1 alone. DNA-polyethyleneimine complexes were removed from cells after 4 h and replaced with fresh DMEM plus 10% FCS containing the following drugs at the concentrations indicated in the figure legends (Figs. 4, 5, and 6): 8-bromoadenosine-3′,5′-cyclic monophosphate (8-Br-cAMP; Sigma), myristoylated protein kinase A-specific inhibitor (peptide residues 14–22 of the heat-stable PKA inhibitor protein, PKI), ribosomal S6 kinase inhibitor (kaempferol-3-*O*-(3″,4″-di-*O*-acetyl-α-L-rhamnopyranoside), SL0101) and InSolution KT5720 protein kinase A inhibitor (all obtained from Calbiochem, VWR International (Leicestershire, UK)).

After overnight incubation with drugs, green fluorescent cells were selected for whole cell patch clamp analysis. Pipette solution was K^+-rich and contained 10 mM NaCl, 117 mM KCl, 2 mM $MgSO_4$, 10 mM HEPES, 11 mM EGTA, 1 mM $CaCl_2$, 2 mM Na_2ATP, pH 7.2, with KOH; free $[Ca^{2+}] = 27$ nM. Bath solution was Na^+-rich and contained 135 mM NaCl, 5 mM KCl, 1.2 mM $MgCl_2$, 5 mM HEPES, 2.5 mM $CaCl_2$, 10 mM D-glucose, pH 7.4, with NaOH. All experiments were carried out at room temperature. Patch pipettes were manufactured from standard walled borosilicate glass capillary tubing (Kwik-Fil, Sarasota, Florida) on a two-stage Narishige PP-83 pipette puller (Narishige Scientific Instrument Laboratory, Kasuya, Tokyo, Japan), were heat-polished on a Narishige microforge, and had measured tip resistances of 4–8 megaohms (when filled with K^+-rich pipette solution). Resistive feedback voltage clamp was achieved using an Axopatch 200 B amplifier (Axon Instruments, Foster City, CA). Voltage protocols were generated, and currents were recorded using pClamp 10.0.5 or pClamp 10 software employing Digidata 1200 (Axon Instruments). Data were filtered (4-pole Bessel) at 1 kHz and digitized at 5 kHz. Following successful transition to the whole-cell recording mode, capacitance transients were compensated for and measured. To evoke ionic currents, a voltage step protocol (−100 to 90 mV in 10-mV increments, 100 ms) was employed, and current-voltage relationships were constructed from the plateau stage of each 100-ms step. Membrane potential recordings were performed using a current clamp protocol.

Flow Cytometry—HEK293 cells were plated in 10-cm dishes, 2×10^6 cells/dish, and transfected transiently with 10 μg of GFP-$rK_{2P}3.1$-HA, GFP-$rK_{2P}9.1$-His, eGFP alone, or empty pcDNA3.1 (Invitrogen), as described above. After overnight incubation, cells were harvested using trypsin, pooled, and replated to obtain a single starting population with the same efficiency of transfection. Cells were next grown in the presence or absence of 8-Br-cAMP (concentration indicated in the figure legend) for 16 h, before harvesting by scraping, staining on ice with mouse monoclonal anti-HA tag antibody (clone 16B12, Covance (Leeds, UK)) at 1:400 dilution, mouse monoclonal anti-His tag (catalog no. 70796-3, Novagen, VWR International, Leicestershire, UK) at 1:400 dilution, an isotype control, or no antibody, followed by goat anti-mouse $F(ab')_2$ fragment conjugated to Alexa Fluor 647 (Invitrogen) at 1:1000 dilution. Cells were then analyzed by flow cytometry using a FACSCanto (BD Biosciences), collecting 10^5 transfected cells or 10^5 cells in total for empty vector samples.

Microscopy—HEK293 cells were transfected transiently with GFP-$rK_{2P}3.1$-HA or eGFP alone, on coverslips, as described above; grown overnight in the presence or absence of drugs; and then fixed with 4% (w/v) formaldehyde in PBS for 7 min at room temperature, blocked with 3% (w/v) BSA in PBS, and stained with anti-HA tag antibody and goat anti-mouse $F(ab')_2$ fragment conjugated to Alexa Fluor 647 as described above. Coverslips were mounted and visualized using a Leica TCS SP5 confocal scanning microscope in the University of Southampton Biomedical Imaging Unit.

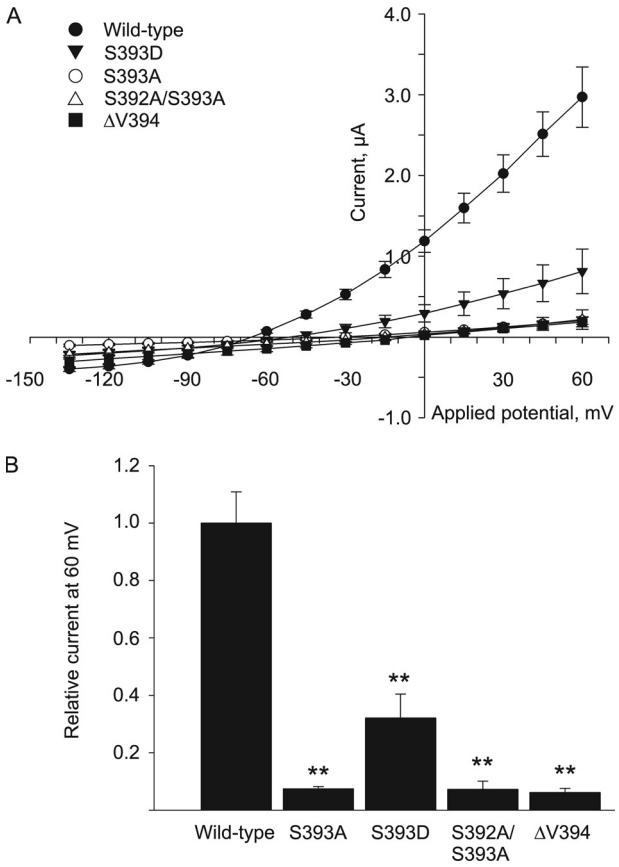

FIGURE 1. **S393 in $hK_{2P}3.1$ is critical for current expression in *Xenopus* oocytes.** *A*, RNA encoding full-length, wild type (●), or mutant $hK_{2P}3.1$ channels was injected into *Xenopus* oocytes, and current was measured by two-electrode voltage clamp. ○, S393A, terminal serine substituted by alanine; ▼, S393D, terminal serine substituted by aspartate; △, S392A/S393A, terminal and penultimate serines both substituted by alanine; ■, ΔV394, final valine removed. *B*, current at 60 mV expressed relative to the wild type $hK_{2P}3.1$ channel. The *asterisks* indicate that the values are significantly different from the wild type (*, $p \leq 0.05$; **, $p \leq 0.01$; ***, $p \leq 0.001$; by Student's *t* test or Mann-Whitney rank sum test). *Error bars*, S.E.

Statistics—Graph and statistical analysis software SigmaPlot 11.0 (Systat Software, Chicago, IL) was used to plot electrophysiology data and perform significance tests. Data were first subjected to the Kolmogorov-Smirnov test for normality. Normal populations were analyzed using Student's *t* test. Non-normal populations were analyzed using the Mann-Whitney rank sum test.

RESULTS

Expression of Functional $hK_{2P}3.1$ in Xenopus Oocytes—Phosphorylation of the terminal serine in the $hK_{2P}3.1$ C terminus is critical for 14-3-3 interaction with the channel (11). Similarly, in $rK_{2P}3.1$, substitution of this serine with an alanine (S410A) causes loss of current and membrane expression in *Xenopus* oocytes (12). We tested the effect of substituting amino acids at the channel C terminus on the function of $hK_{2P}3.1$ expressed in *Xenopus* oocytes (Fig. 1*A*). Substituting the terminal serine for alanine (S393A) resulted in a total loss of current, as did either the double substitution S392A/S393A or the removal of the terminal valine residue (ΔV394). These mutations are known to result in the abrogation of 14-3-3 binding (11, 12, 15) and thus prevent the channel from being correctly targeted to the plasma membrane. Of interest, no significant difference in current expression of the channel was observed when S392A substitution was performed (data not shown); this is in agreement with previous reports, which propose that this residue is not critical to 14-3-3 binding (11). Substitution of the terminal serine for aspartate (S393D), in an attempt to mimic the negative charge of a phosphoserine residue, restored some current (0.81 μA at 60 mV, S.E. = 0.28, $n = 6$ *versus* the control (2.97 μA, S.E. = 0.37, $n = 4$)). Fig. 1*B* shows the surface current expressed in *Xenopus* oocytes at 60 mV for each mutant channel relative to wild type $hK_{2P}3.1$. The reduction in current expression for each of the mutants is significant ($p \leq 0.01$ by Student's *t* test or Mann-Whitney rank sum test), confirming the critical nature of the terminal serine of $hK_{2P}3.1$ for functional channel expression. Currently, the kinase responsible for phosphorylating this residue is unknown.

Phosphorylation of $hK_{2P}3.1$ and $hK_{2P}9.1$—We analyzed the sequences of human and rat $K_{2P}3.1$ and $K_{2P}9.1$ using the NetPhosK 1.0 server (Danish Technical University) (18) to predict candidate kinases for Ser^{393} ($hK_{2P}3.1$), Ser^{410} ($rK_{2P}3.1$), Ser^{373} ($hK_{2P}9.1$), and Ser^{395} ($rK_{2P}9.1$) (Table 2). For all channels, PKA was predicted as the most likely candidate to phosphorylate the terminal serine (predicted score range = 0.87–0.89; maximum score = 1.0); RSK and PKC were predicted with much lower probabilities (RSK predicted score range = 0.61–0.70; PKC predicted score range 0.68–0.74; Table 2). The C-terminal 15 residues of $K_{2P}3.1$ contain an additional serine residue, Ser^{392} ($hK_{2P}3.1$) or Ser^{409} ($rK_{2P}3.1$), and this also conforms to the known site specificity for PKA. However, Ser^{409} is not required for surface expression of $rK_{2P}3.1$ (12) (data not shown), as demonstrated by substitution of Ser^{392} by alanine causing no significant inhibition of channel current when expressed in *Xenopus* oocytes. Aside from the terminal serine residues, C-terminal residues Ser^{382} and Thr^{383} in $hK_{2P}3.1$ are predicted to be phosphorylated by PKC and cyclin-dependent kinase 2, respectively, and Thr^{400} of $rK_{2P}3.1$ is predicted to be phosphorylated by PKC (Table 2).

To determine if the predicted kinase could phosphorylate the terminal serine of these channels, the C-terminal 15 amino acids of each channel fused to GST were expressed in *E. coli*. We conducted *in vitro* phosphorylation assays using crude lysate supernatant as a substrate and recombinant purified PKA, RSK2, and PKCα. RSK2 was chosen because it exhibits the tissue distribution pattern most similar to those of $K_{2P}3.1$ and $K_{2P}9.1$ (14, 19–22). We also selected two serine/threonine-specific kinases, MAPK I (ERK1) and casein kinase II, which were not predicted to phosphorylate the C-terminal motifs. Fig. 2 shows the purified fusion proteins after separation by standard (*A* and *C*) and Phos-tag (*B* and *D*) SDS-PAGE, a non-radioactive technique that reduces the electrophoretic mobility of phosphorylated proteins relative to their non-phosphorylated counterparts (23).

PKA phosphorylated GST-$hK_{2P}3.1$ (Fig. 2*D*), as shown by the upward bandshift relative to the control incubations of the fusion proteins without kinase (Fig. 2*D*, *Con lane*) and relative to GST alone (Fig. 2*B*). For $hK_{2P}3.1$, there are three distinct bands (Fig. 2*D*, *PKA lane*). The first (marked *0P*) migrates at a position corresponding to the fusion protein incubated without

TABLE 2

Phosphorylation sites in the C-terminal 15 amino acids of $K_{2P}3.1$ and $K_{2P}9.1$, as predicted by the NetPhosK 1.0 server

The serine residue critical for forward transport of the channels is shown in boldface type. In $K_{2P}3.1$, other potentially phosphorylated residues are underlined. CKI, casein kinase I; CDC2, cyclin-dependent kinase 2; PKG, protein kinase G. Scores over 0.5 indicate a potential phosphorylation site. The maximum score is 1.0.

		NetPhosK 1.0 phosphorylation prediction		
Channel	Sequence of C terminus	Residue	Kinase	Score (cut-off = 0.5, maximum = 1.0)
$K_{2P}3.1$ human	^{380}SLSTFRGLMKRRS**S**V^{394}	**Ser^{393}**	PKA	0.88
			PKC	0.74
			RSK	0.67
		Ser^{392}	PKA	0.75
		Thr^{383}	PKC	0.90
			CKI	0.54
		Ser^{382}	CDC2	0.53
$K_{2P}3.1$ rat	^{397}SLATFRGLMKRRS**S**V^{411}	**Ser^{410}**	PKA	0.88
			PKC	0.72
			RSK	0.70
		Ser^{409}	PKA	0.76
		Thr^{400}	PKC	0.88
$K_{2P}9.1$ human	^{360}SFTDHQRLMKRRK**S**V^{374}	**Ser^{373}**	PKA	0.89
			RSK	0.68
			PKC	0.68
			PKG	0.53
$K_{2P}9.1$ rat	^{382}TCGENHRLHIRRK**S**I^{396}	**Ser^{395}**	PKA	0.87
			RSK	0.61

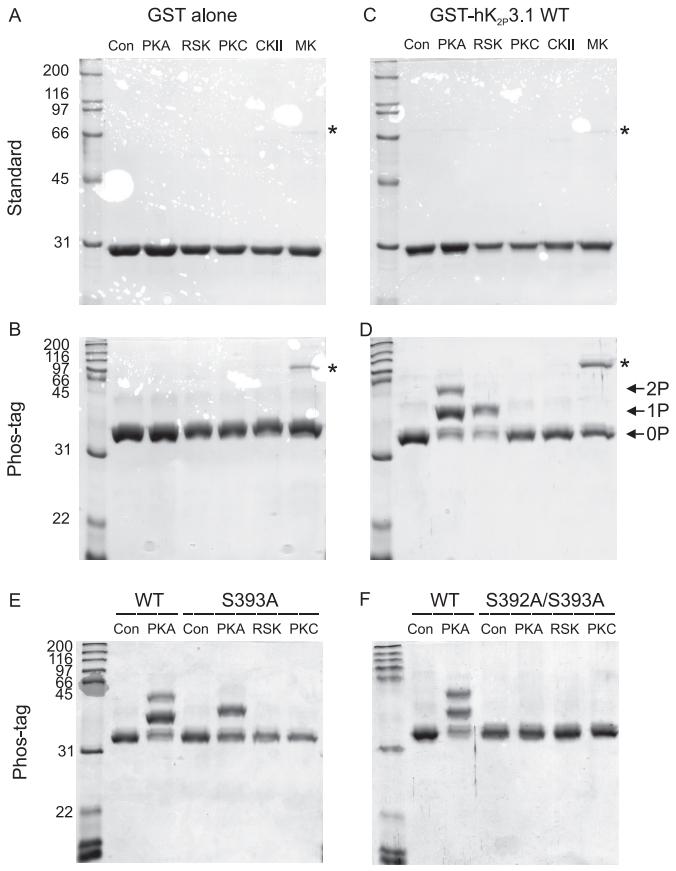

FIGURE 2. **PKA and RSK phosphorylate $K_{2P}3.1$ at Ser^{393} *in vitro*.** Lysates of *E. coli* expressing fusion proteins were added to ATP and purified kinases, and then the fusion proteins were purified using glutathione-Sepharose. Purified proteins were subjected to either standard or Phos-tag SDS-PAGE, as indicated to the *left*, and then stained with Coomassie Blue. *Con*, control (no kinase); *CKII*, casein kinase II; *MK*, MAPK I. As a control, GST alone was incubated with the purified kinases (*A* and *B*). *C* and *D*, wild type $K_{2P}3.1$ C terminus. *Bands* marked *1P* and *2P* represent single- and double-phosphorylated proteins, respectively. The *band* marked with an *asterisk* is most likely to be co-purifying MAPK I. *E*, $K_{2P}3.1$ wild type (SSV) compared with mutant S393A (SAV). Panel *F*, $K_{2P}3.1$ wild type (SSV) compared with S392A/S393A (AAV).

kinase (*Con lane*), which represents a population of unphosphorylated fusion proteins. The second band (marked *1P*) corresponds to a population of molecules stoichiometrically phosphorylated at a single serine, whereas the third population (*2P*) is phosphorylated at both serines. That the respective band shifts are due to phosphorylation of GST-$hK_{2P}3.1$ at Ser^{392} and Ser^{393} is confirmed by the loss of the uppermost band in the mutant S393A, where the terminal serine has been mutated to the non-phosphorylatable alanine (Fig. 2*E*, *S393A*, *PKA lane*) and both bands in S392A/S393A (Fig. 2*F*, *S392A/S393A*, *PKA lane*). RSK2 phosphorylated the majority of GST-$hK_{2P}3.1$ at a single serine; this was abolished in the mutant S393A. By contrast, any phosphorylation of GST-$hK_{2P}3.1$ by PKCα is at the limit of detection, although the enzyme does phosphorylate a control substrate histone H1 (supplemental Fig. 1). Thus, *in vitro*, PKCα does not appreciably phosphorylate either Ser^{393} or indeed Ser^{382}, the second residue in the C-terminal 15 amino acids of $hK_{2P}3.1$ predicted to be a target for PKC. Negative control kinases MAPK and casein kinase II also failed to phosphorylate the fusion proteins but were active when presented with an appropriate substrate (supplemental Fig. 1).

We performed similar assays with both GST-$hK_{2P}9.1$ and GST-$rK_{2P}9.1$ (Fig. 3, *A* and *B*). In the presence of PKA, all of the fusion protein migrates more slowly than the control, indicative of phosphorylation-dependent decreased motility through the Phos-tag gel. By contrast, RSK2 phosphorylated only a minor proportion of the human and rat fusion proteins, and PKCα phosphorylated almost none at all. When the terminal serine residues were mutated to alanine (*C*, S373A ($hK_{2P}9.1$); *D*, S395A ($rK_{2P}9.1$)), no phosphorylation by PKA, RSK2, or PKCα was detected (a corollary of which is that any phosphorylation by PKCα is not at residue Thr^{400}). Thus, *in vitro* assays support the NetPhosK prediction that PKA is a good candidate to phosphorylate the terminal serine of both $hK_{2P}3.1$ and human and rat $K_{2P}9.1$. However, of the small panel of kinases tested, RSK2 is also able to phosphorylate the terminal serine of $hK_{2P}3.1$ effectively *in vitro*.

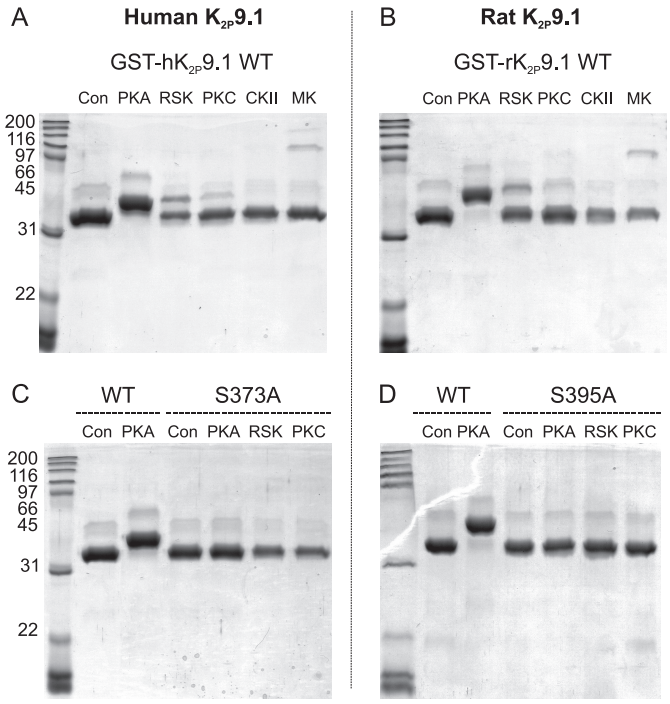

FIGURE 3. **PKA phosphorylates both human and rat $K_{2P}9.1$ C-terminal forward transport motifs *in vitro*.** *In vitro* phosphorylation of C terminus fused to GST. Lysates of *E. coli* expressing fusion proteins were spiked with ATP and purified kinases, and then the fusion proteins were purified using glutathione-Sepharose. Purified proteins were separated by Phos-tag SDS-PAGE. Kinases were as described in the legend to Fig. 2. *A* and *B*, human and rat wild type $K_{2P}9.1$, respectively. *C*, human $K_{2P}9.1$ wild type (KSV) compared with mutant S373A (KAV). *D*, rat $K_{2P}9.1$ wild type (KSV) compared with mutant S395A (KAI). *Con*, control (no kinase); *CKII*, casein kinase II; *MK*, MAPK I.

Sensitivity of Membrane Expression of $hK_{2P}3.1$ to Kinase-modulating Drugs—To test whether phosphorylation by PKA and RSK2 regulates plasma membrane targeting of $hK_{2P}3.1$, the channel was transiently expressed in HEK293 cells, in the presence and absence of the PKA activator, 8-Br-cAMP; two PKA inhibitors, myristoylated PKI (a specific inhibitor of PKA catalytic subunit) and the small molecule KT5720; or a highly specific RSK inhibitor, SL0101, which binds to an adenosine-interacting loop that is unique to RSK and differs markedly from other kinases, including PKA (24). Transfected cells were identified by co-transfecting GFP in a separate plasmid and selecting green fluorescent cells. $K_{2P}3.1$ is constitutively active at the cell surface, so measured K^+ flux is directly proportional to the number of channels inserted in the plasma membrane. We determined the current passed in transfected cells at different applied potentials, using whole-cell patch clamp (Fig. 4). Cells transfected with WT-$K_{2P}3.1$ (plus pEGFP-C1) show a negative shift in resting membrane potential from −32.6 mV (S.E. = 1.16, $n = 6$) in non- or pEGFP-C1 transfected cells to −54.6 mV (S.E. = 3.12, $n = 14$) in cells transfected with the channel. Currents evoked by step depolarization from −100 to +90 mV showed instantaneous outward currents, with a small time-dependent component, non-inactivating outward current, with a reversal potential negative of −50 mV typical of $K_{2P}3.1$. Currents also showed characteristic sensitivity to external acidosis (data not shown). For cells transfected with $hK_{2P}3.1$ and cultured in the presence of 0.4 mM 8-Br-cAMP (Fig. 4*A*), increased current was observed at test potentials between −50 mV and +90 mV. At 60 mV, evoked current increased from 0.59 nA (S.E. = 0.05, $n = 7$) to 1.09 nA (S.E. = 0.14, $n = 9$) in 8-Br-cAMP treated cells, with an associated modest negative shift in the resting membrane potential to −58.6 mV (S.E. = 2.45, $n = 7$). The effect of PKA enhancement by 8-Br-cAMP on serine-substituted channels S393A and S393D was also examined. HEK293 cells transfected with either $hK_{2P}3.1$ S393A or S393D failed to express whole-cell currents significantly different from that of non-transfected cells; furthermore, treatment with 0.4 mM 8-Br-cAMP failed to enhance whole cell currents of non-transfected HEK293 cells or HEK293 cells transfected with either of the two phosphorylation mutant channels (Fig. 4*B*).

Unexpectedly, the RSK inhibitor, SL0101, causes an increase in current (1.01 nA, S.E. = 0.12, at 60 mV, $n = 8$; Fig. 4*A*) although without a concomitant decrease in membrane potential (V_m for RSK-treated cells was −37.9 mV; S.E. = 2.05 mV; $n = 5$) compared with non-treated matched controls (−47.4 mV, S.E. = 4.47, $n = 5$), suggesting that RSK inhibition may have either nonspecific effects on other channels expressed in HEK293 or additional (direct or indirect) regulatory effects on $K_{2P}3.1$. In addition, a nonspecific target of SL0101 might explain these data.

In a separate experiment (Fig. 4*C*), the effects of two different PKA inhibitors on current expression in HEK293 cells transfected with $hK_{2P}3.1$ were tested. Transfected cells were cultured in the presence of either 1 μM KT5720 or 20 μM PKI for 16 h prior to whole-cell voltage clamp analysis. Both PKA inhibitors resulted in a decrease in current at all test potentials when compared with non-treated cells. Non-treated $hK_{2P}3.1$-transfected cells passed 1.15 nA (S.E. = 0.08, $n = 8$) of current at 60 mV, whereas cells treated with 1 μM KT5720 or 20 μM PKI showed reduced current of 0.81 nA (S.E. = 0.09, $n = 6$) and 0.67 nA (S.E. = 0.06, $n = 9$) at the same test potential. Statistical analysis indicates that all drug treatments are significantly different from the untreated control ($p \leq 0.05$; Fig. 4*D*). Similarly, $hK_{2P}3.1$ and $hK_{2P}9.1$ channels expressed in *Xenopus* oocytes demonstrated inhibition of their current by PKI comparable with that seen for these channels in HEK293 cells, with statistical analysis indicating that PKI treatment was significantly different from untreated controls ($p \leq 0.014$ for $hK_{2P}3.1$ and $p \leq 0.002$ for $hK_{2P}9.1$; supplemental Fig. 2). Taken together, our data provide strong evidence that functional PKA is necessary for plasma membrane expression of $hK_{2P}3.1$.

Immunofluorescence of Tagged $K_{2P}3.1$—We next sought to corroborate our cellular observations using confocal microscopy. HEK293 cells were transfected with $rK_{2P}3.1$ fused at the N terminus to eGFP and incorporating a non-interfering HA tag in an external loop of the second pore-forming domain (GFP-$rK_{2P}3.1$-HA). The external tag made it possible to compare the relative amounts of channel expressed at the cell surface under different conditions by staining with anti-tag antibodies. Transfected cells were incubated with 8-Br-cAMP or PKA inhibitors and then fixed (but not permeabilized) and stained with anti-HA tag antibody (Fig. 5). In control cells (Fig. 5, *A–C*), anti-HA staining (Fig. 5*B*, *red*) can be seen around the periphery of a subset of transfected cells; not all green fluorescent cells display detectable tagged channel on the plasma membrane, suggesting that aberrant folding and/or targeting of the

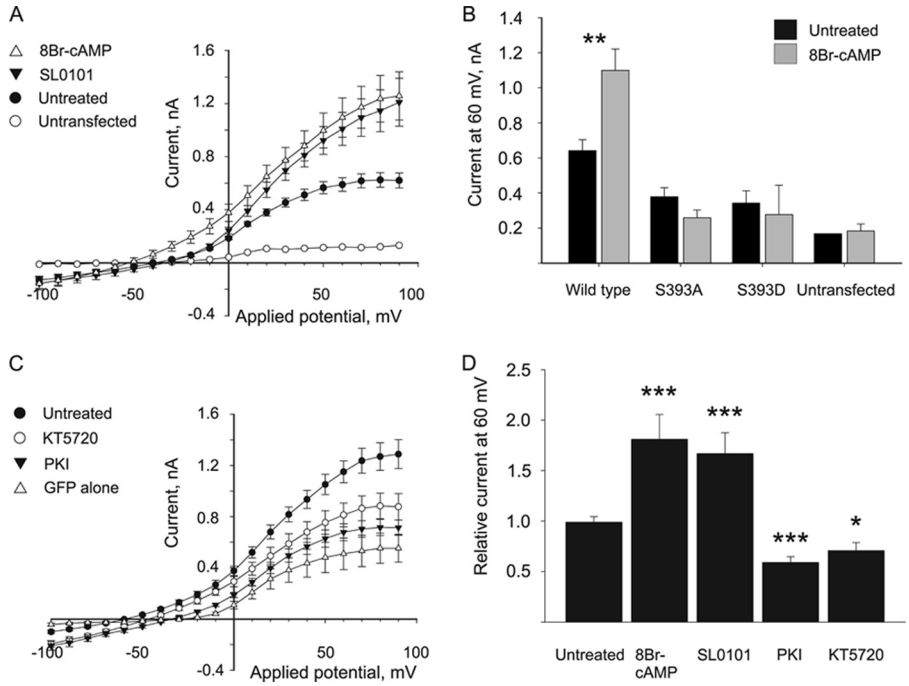

FIGURE 4. **Modulation of PKA or RSK kinase activity affects wild type $K_{2P}3.1$ current in HEK293 cells.** Cells co-transfected with $K_{2P}3.1$ and GFP on separate plasmids were grown with or without kinase inhibitor or activator compounds, and then surface currents were measured by whole-cell patch clamp analysis. *A*, cells were incubated in the presence of 0.4 mM 8-Br-cAMP (PKA activator; △), 50 μM SL0101 (RSK inhibitor; ▼), or DMSO (untreated control; ●). ○, non-transfected cells. *B*, effect of 8Br-cAMP on wild type $hK_{2P}3.1$ compared with mutants S393A and S393D in HEK293 cells. Plot shows current at 60 mV with and without 8Br-cAMP. *C*, cells were incubated in the presence of 1 μM KT5720 (PKA inhibitor; ○), 20 μM PKI (PKA inhibitor; ▼), or DMSO (untreated control; ●). △, GFP alone. *D*, current at 60 mV, with or without inhibitors or activators from *A* and *C*, expressed relative to the untreated control. The *asterisks* indicate that the values are significantly different from the untreated control (*, $p \leq 0.05$; **, $p \leq 0.01$; ***, $p \leq 0.001$; by Student's *t* test or Mann-Whitney rank sum test). *Error bars*, S.E.

tagged channel may take place when expressed in HEK293 cells. In the presence of 8-Br-cAMP (Fig. 5, *D–F*), more HA-positive cells could be observed over multiple fields of view, and these cells stained more brightly than control cells. By contrast, when cells were incubated with PKA inhibitors KT5720 (Fig. 5, *G–I*) or PKI (*J–L*), anti-HA staining was weaker. In the presence of the RSK inhibitor SL0101 (Fig. 5, *M–O*), anti-HA staining was comparable or slightly brighter than the control. Cells transfected with eGFP-C1 alone were not markedly affected by the drugs (supplemental Fig. 3). Therefore, immunofluorescence evidence supports both the *in vitro* and functional evidence that PKA is the central kinase that regulates forward transport of $K_{2P}3.1$.

Effect of PKA Activation on Surface Expression of Tagged $K_{2P}3.1$ and $K_{2P}9.1$ Channels—To obtain a quantitative measure of the effect of activating PKA on the surface expression of both $K_{2P}3.1$ and $K_{2P}9.1$, we used the rat variants of these channels with GFP fused to the channel N terminus and either an HA tag ($K_{2P}3.1$) or His tag ($K_{2P}9.1$) in the external loop of the second pore-forming domain (GFP-$rK_{2P}3.1$-HA and GFP-$rK_{2P}9.1$-His, respectively). HEK293 cells were transiently transfected with either one of the tagged channel constructs, eGFP-C1 alone or empty vector, and surface expression was analyzed by flow cytometry (Fig. 6). After transfection, cells were incubated overnight with or without 0.4 mM 8-Br-cAMP to activate PKA. Fig. 6*A* shows the distribution of GFP fluorescence (*i.e.* total expression of GFP-$hK_{2P}3.1$-HA fusion protein within the cell population). The peaks under the horizontal marker represent transfected cells, as judged by analysis of cells transfected with vector alone and eGFP-C1 alone (supplemental Fig. 4). Activation of PKA with 8-Br-cAMP results in a relative increase in the number of brightly fluorescent cells (Fig. 6*A*, *black line*).

To determine the level of GFP-$rK_{2P}3.1$-HA channel expressed at the plasma membrane, 10^5 transfected cells from each treatment (green fluorescent cells, defined by the marker in Fig. 6*A*; see also supplemental Fig. 4) were compared for binding of anti-HA antibody (*B*, far red fluorescence). In agreement with the immunofluorescence data above, not all transfected cells stain positive for the externally facing HA tag. In this experiment, activation of PKA by 8-Br-cAMP treatment results in a 27% increase in the number of HA-positive cells relative to the control. There is an accompanying slight increase in the mean fluorescence intensity from 2036 (control) to 2206 (8-Br-cAMP) arbitrary fluorescence units compared with the control (an 8% increase in mean fluorescence intensity). 8-Br-cAMP treatment did not increase the expression of GFP alone; nor did it alter the background fluorescence of cells transfected with empty vector (supplemental Fig. 4).

A similar pattern emerged for GFP-$rK_{2P}9.1$-His surface expression in response to 8-Br-cAMP treatment. A 53% increase in the proportion of transfected cells that express detectable channel at the plasma membrane was detected as well as a 20% increase in mean fluorescence intensity from 740 to 890 arbitrary fluorescence units (Fig. 6*D*). From these observations, we conclude that activating PKA promotes forward transport of both $K_{2P}3.1$ and $K_{2P}9.1$ channels.

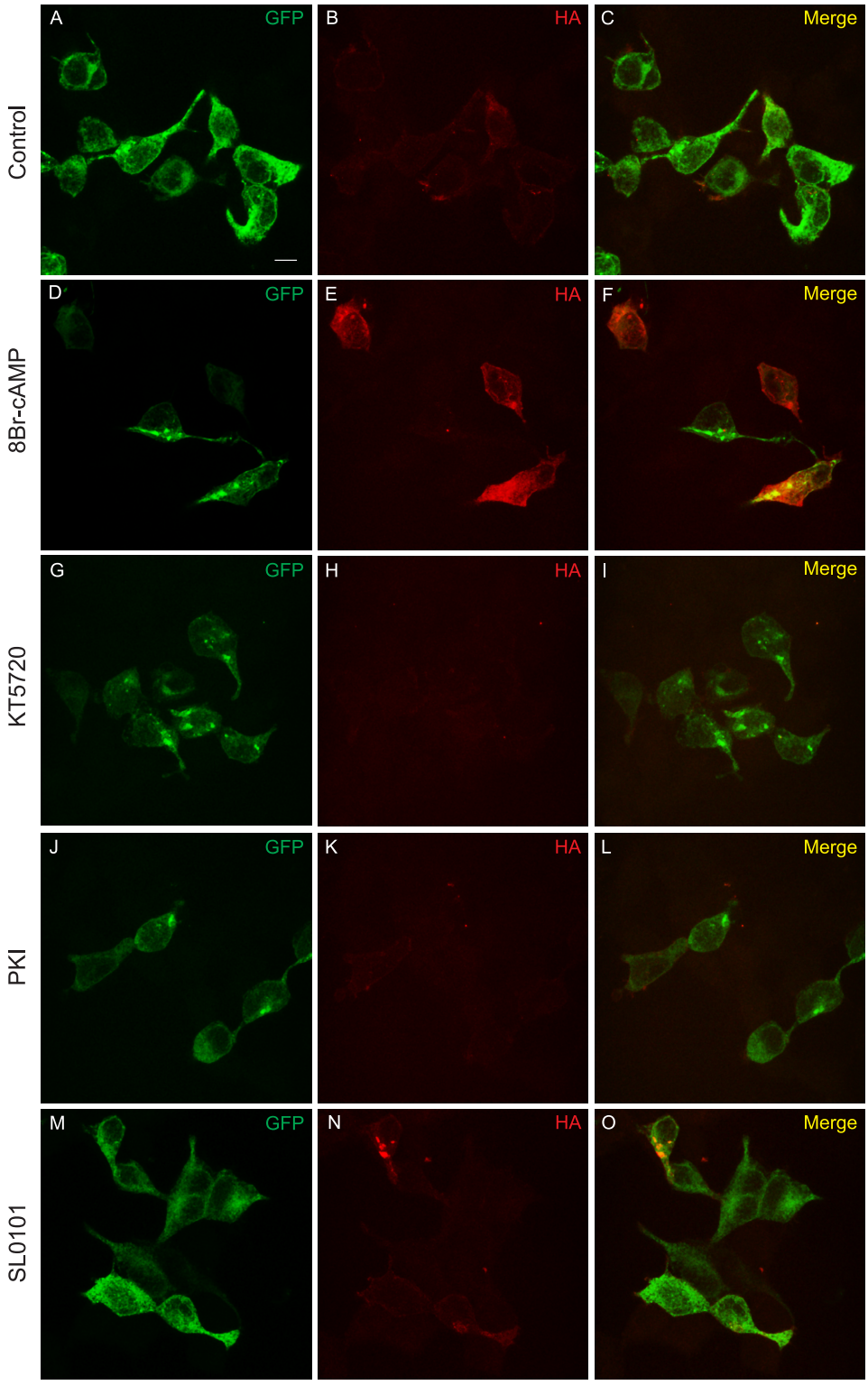

FIGURE 5. **Immunostaining shows PKA activation results in increased surface expression of $K_{2P}3.1$.** Cells transfected with GFP-K_{2P}3.1-HA were grown in the presence of DMSO (control; *A–C*), 50 μM 8Br-cAMP (*D–F*), 1 μM KT5720 (*G–I*), 20 μM PKI (*J–L*), or 50 μM SL0101 (*M–O*) and then fixed and stained with anti-HA tag antibody and an Alexa Fluor 647-conjugated secondary antibody. The cells were not permeabilized, so only surface-exposed HA tag in correctly targeted channel was accessible to the antibody. Images are a confocal *z*-stack. *GFP*, total expression of the fusion protein; *HA*, surface-exposed HA tag; *Merge*, composite image. *Scale bar* (*A*), 10 μm.

DISCUSSION

Precise control of cell surface expression of the acid-sensitive K_{2P} channels, $K_{2P}3.1$ and $K_{2P}9.1$, is critically important in the control of membrane potential in both excitable and non-excitable cells. Here, we used bioinformatic analysis, *in vitro* assays, and recombinant functional assays to elucidate the kinase responsible for control of forward transport of these channels.

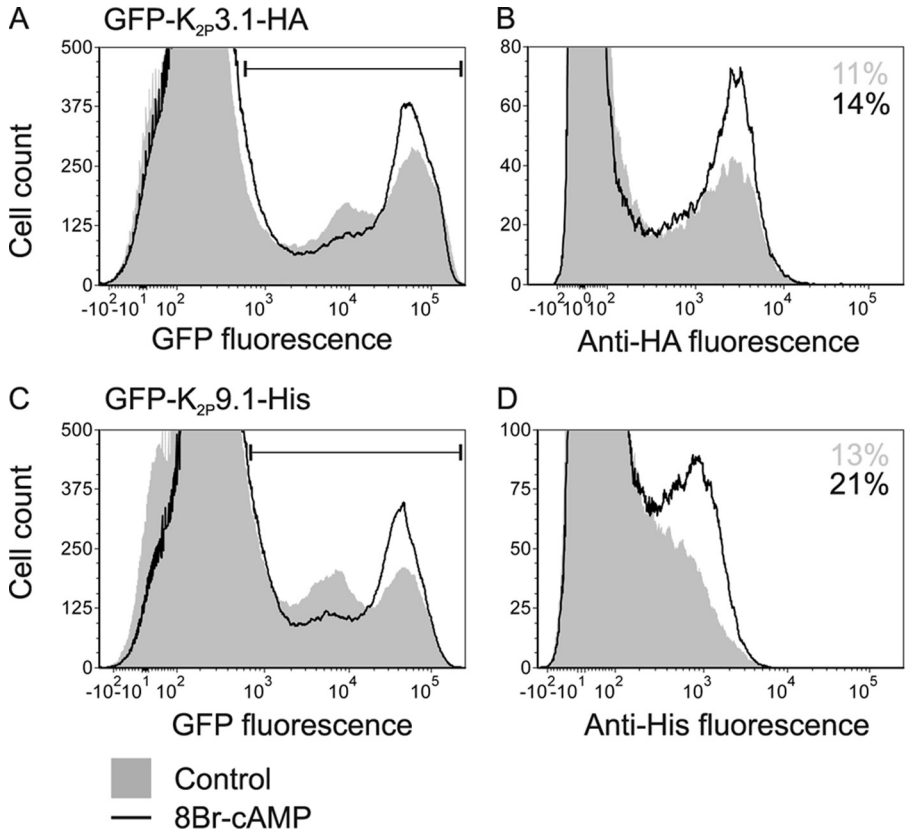

FIGURE 6. **Activation of PKA increases the number of $K_{2P}3.1$ and $K_{2P}9.1$ on the cell surface.** Cells transfected with GFP-K_{2P}3.1-HA or GFP-K_{2P}9.1-His were grown in the presence or absence of the PKA activator 8Br-cAMP (0.4 mM) and then harvested and stained with anti-tag antibodies and an Alexa Fluor 647-conjugated secondary antibody before analysis by flow cytometry. *A*, GFP-K_{2P}3.1-HA, total expression as measured by GFP fluorescence. *Shaded area*, control; *black line*, 8-Br-cAMP. The *horizontal marker* indicates GFP-positive, transfected cells. *B*, 10^5 transfected cells from *A* were analyzed for surface expression of the channel, as detected by binding of antibody to the external HA tag. The *numbers* denote the proportion of transfected cells that stain positive for the HA tag. *C*, GFP-K_{2P}9.1-His, total expression as measured by GFP fluorescence. *D*, 10^5 transfected cells from *C* were analyzed for surface expression of the channel, as detected by binding of antibody to the external His tag. The *numbers* denote the proportion of transfected cells that stain positive for the His tag.

The C termini of both $K_{2P}3.1$ and $K_{2P}9.1$ contain a number of residues that are predicted targets for modulation by phosphorylation. Among these, some residues are already identified as being phosphorylated and playing a role in channel modulation, including PKC activation resulting in a 40% decrease in murine $K_{2P}3.1$ current over a 30-min time course (4). Also, $hK_{2P}9.1$ contains a C-terminal threonine (Thr^{341}), which is a target for phosphorylation by PKC, with a resultant reduction in current amplitude (25). In 2002, we and others identified a phosphorylation-dependent forward transport pathway for $K_{2P}3.1$, which has subsequently been shown to be utilized by $K_{2P}9.1$ and a number of other proteins. Phosphorylation of the terminal serine of the acid-sensitive K_{2P} channels was shown to result in recruitment of 14-3-3, which we demonstrated to be critical for channel forward transport (11, 12, 14). 14-3-3 has also been shown to play a role in the intracellular transport of a number of other membrane proteins, including the K_{ATP} channel Kir6.2, invariant chain protein, nicotinic acetylcholine receptor (nAChRα4), kainate receptor KA2, and G-protein-coupled receptor 15 (11, 26). Furthermore, another K_{2P} channel member (K_{2P}18.1/TRESK) has recently been shown to be negatively regulated by 14-3-3 in a phosphorylation-dependent manner (27).

Serine substitution and targeted phosphorylation of peptides analogous to the terminal residues of $K_{2P}3.1$ demonstrated the critical nature of the terminal serine (and its phosphorylation) to 14-3-3 recruitment (11, 12). Here, we build upon the previously reported biochemical evidence by providing functional confirmation of the importance of the terminal serine (Ser^{393}) in $hK_{2P}3.1$. Mutation of the Ser^{393} to alanine, which can neither be phosphorylated nor mimic a phosphorylated residue, resulted in the channel failing to pass current when expressed in *Xenopus* oocytes. This correlates well with reports from Rajan *et al.* (12) for an equivalent residue (Ser^{410}) in the rat homolog.

To understand the physiological mechanism and signaling pathways that enable regulation of cell surface expression of $K_{2P}3.1$, it is crucial to identify the kinase responsible for phosphorylation of the serine critical to 14-3-3 recruitment (Ser^{393} in $hK_{2P}3.1$). Prior to this study, the identity of this kinase was unknown. Here we use algorithms to predict the kinases most likely to phosphorylate the C-terminal forward transport motif of the acid-sensitive channels ($hK_{2P}3.1$, $rK_{2P}3.1$, $hK_{2P}9.1$, and $rK_{2P}9.1$) and then exploit a combination of approaches to directly test these predictions: kinase assays to determine the ability of each kinase to phosphorylate the site *in vitro*, patch clamp analysis of HEK293 cells expressing $hK_{2P}3.1$ to determine K^+ current in the presence of kinase-modulating drugs, and immunofluorescence and flow cytometry to measure and quantify changes in the surface expression of channel in response to activating or inhibiting specific kinases.

For human and rat $K_{2P}3.1$ and $K_{2P}9.1$, PKA was predicted and subsequently demonstrated to be the most likely kinase to phosphorylate the terminal serine. Through serine substitution and mutation analysis, we further demonstrated that phosphorylation of the C-terminal fusion proteins was lost upon substitution of the terminal serine (Figs. 2 and 3). Two interesting observations were borne out by the *in vitro* kinase assays. (i) We observed that the ribosomal S6 kinase, RSK2, phosphorylated the $hK_{2P}3.1$ C-terminal fusion protein as effectively as PKA *in vitro* (Fig. 2). (ii) *In vitro* phosphorylation analysis also detected phosphorylation of Ser^{392} of $hK_{2P}3.1$ by PKA. Ser^{392} has previously been shown not to be required for 14-3-3 recruitment and hence forward transport of the channel (11, 12). Patch clamp analysis, flow cytometry, and immunocytochemistry studies of HEK293 transfected with WT $hK_{2P}3.1$ and cultured in the presence of PKA activators or inhibitors all confirm that activation of PKA resulted in an increase in $hK_{2P}3.1$ current expression (Figs. 4–6) and demonstrate the dynamic regulatory effect of PKA activity on $K_{2P}3.1$ channel expression.

RSK2 phosphorylated $hK_{2P}3.1$ at the critical serine (Ser^{393}) in our *in vitro* studies, and we hypothesized that if RSK2 phosphorylation was critical to Ser^{393} phosphorylation and hence forward transport of the channel, a reduction in $hK_{2P}3.1$ current is predicted in response to RSK2 inhibition. In contrast, we observed that current expression in cells transfected with $hK_{2P}3.1$ was increased when they were treated with the RSK inhibitor SL0101. Although this finding was unexpected, it does demonstrate that RSK phosphorylation of the channel is not critical for the channel to achieve cell surface expression. A number of potential explanations of the observed increase in $K_{2P}3.1$ current expression exist, including a role of RSK in acute channel modulation following cell surface expression of the channel. In this study, we focused on a single phosphorylation site known to be important in cell surface expression of $K_{2P}3.1$. However, a second non-related serine (Ser^{334} in $hK_{2P}3.1$) is also predicted to be phosphorylated by RSK, and this site could have additional modulatory roles on channel function. Furthermore, RSKs modulate the activity of K^+ currents in both mouse ventricular myocytes and HEK293 cells. In both cases, currents were inhibited by co-expression of RSK (28). Consequently, it is possible that the increased whole-cell currents observed in response to RSK inhibition in this study are due to altered modulation of endogenous current. Moreover, evidence suggests that RSK may have an inhibitory effect on PKA (29). Hence, inhibition of RSK may simply alleviate constitutive inhibition of PKA, resulting in an apparent increase in PKA activity and an increase in channel expression. Immunofluorescence in HEK293 cells transfected with GFP-$rK_{2P}3.1$-HA, however, did not reveal an appreciable increase in the levels of this fusion protein at the plasma membrane after SL0101 treatment. Further experiments are necessary to determine the nature of the K^+ flux in HEK293 cells in response to RSK inhibition.

Therefore, from the data presented in this work, we conclude that *in vivo* expression of $hK_{2P}3.1$ can be modulated by drugs and kinases that activate or inhibit PKA; that activation of PKA leads to phosphorylation of the 14-3-3 C-terminal binding site; and that phosphorylation of a single critical serine is responsible for an increased current. Several hormones and growth factors induce the activation of adenylate cyclase *in vivo*, which, via generation of cAMP, liberates the PKA catalytic subunit from its inactive tetrameric form. Further studies are now required to uncover the signal transduction mechanisms involved in PKA and hence channel activation. It is likely that these will demonstrate some level of tissue specificity, but further studies will provide valuable information on the biology of these channels, whose exact function remains largely unknown, despite their widespread distribution and their implication in numerous physiological and pathophysiological roles.

Acknowledgments—We thank K. Wilkinson, Dr. E. Lowry, Dr. D. A. Johnston, and Prof. S. A. N. Goldstein for contributions to this work.

REFERENCES

1. Enyedi, P., and Czirják, G. (2010) *Physiol. Rev.* **90,** 559–605
2. Patel, A. J., Honoré, E., Lesage, F., Fink, M., Romey, G., and Lazdunski, M. (1999) *Nat. Neurosci.* **2,** 422–426
3. Kindler, C. H., Yost, C. S., and Gray, A. T. (1999) *Anesthesiology* **90,** 1092–1102
4. Lopes, C. M., Gallagher, P. G., Buck, M. E., Butler, M. H., and Goldstein, S. A. (2000) *J. Biol. Chem.* **275,** 16969–16978
5. Buckler, K. J., Williams, B. A., and Honore, E. (2000) *J. Physiol.* **525,** 135–142
6. Sirois, J. E., Lei, Q., Talley, E. M., Lynch, C., 3rd, and Bayliss, D. A. (2000) *J. Neurosci.* **20,** 6347–6354
7. Czirják, G., Fischer, T., Spät, A., Lesage, F., and Enyedi, P. (2000) *Mol. Endocrinol.* **14,** 863–874
8. Talley, E. M., Lei, Q., Sirois, J. E., and Bayliss, D. A. (2000) *Neuron* **25,** 399–410
9. Duprat, F., Lauritzen, I., Patel, A., and Honoré, E. (2007) *Trends Neurosci.* **30,** 573–580
10. Bayliss, D. A., and Barrett, P. Q. (2008) *Trends Pharmacol. Sci.* **29,** 566–575
11. O'Kelly, I., Butler, M. H., Zilberberg, N., and Goldstein, S. A. (2002) *Cell* **111,** 577–588
12. Rajan, S., Preisig-Müller, R., Wischmeyer, E., Nehring, R., Hanley, P. J., Renigunta, V., Musset, B., Schlichthörl, G., Derst, C., Karschin, A., and Daut, J. (2002) *J. Physiol.* **545,** 13–26
13. Girard, C., Tinel, N., Terrenoire, C., Romey, G., Lazdunski, M., and Borsotto, M. (2002) *EMBO J.* **21,** 4439–4448
14. O'Kelly, I., and Goldstein, S. A. (2008) *Traffic* **9,** 72–78
15. Zuzarte, M., Heusser, K., Renigunta, V., Schlichthörl, G., Rinné, S., Wischmeyer, E., Daut, J., Schwappach, B., and Preisig-Müller, R. (2009) *J. Physiol.* **587,** 929–952
16. van Heusden, G. P. (2009) *Genomics* **94,** 287–293
17. Coblitz, B., Wu, M., Shikano, S., and Li, M. (2006) *FEBS Lett.* **580,** 1531–1535
18. Blom, N., Sicheritz-Pontén, T., Gupta, R., Gammeltoft, S., and Brunak, S. (2004) *Proteomics* **4,** 1633–1649
19. Alcorta, D. A., Crews, C. M., Sweet, L. J., Bankston, L., Jones, S. W., and Erikson, R. L. (1989) *Mol. Cell Biol.* **9,** 3850–3859
20. Moller, D. E., Xia, C. H., Tang, W., Zhu, A. X., and Jakubowski, M. (1994) *Am. J. Physiol.* **266,** C351–C359
21. Medhurst, A. D., Rennie, G., Chapman, C. G., Meadows, H., Duckworth, M. D., Kelsell, R. E., Gloger, I. I., and Pangalos, M. N. (2001) *Mol. Brain Res.* **86,** 101–114
22. Roberts, N. A., Haworth, R. S., and Avkiran, M. (2005) *Br. J. Pharmacol.* **145,** 477–489
23. Kinoshita, E., Kinoshita-Kikuta, E., Takiyama, K., and Koike, T. (2006) *Mol. Cell Proteomics* **5,** 749–757
24. Smith, J. A., Poteet-Smith, C. E., Xu, Y., Errington, T. M., Hecht, S. M., and Lannigan, D. A. (2005) *Cancer Res.* **65,** 1027–1034
25. Veale, E. L., Kennard, L. E., Sutton, G. L., MacKenzie, G., Sandu, C., and Mathie, A. (2007) *Mol. Pharmacol.* **71,** 1666–1675
26. Mrowiec, T., and Schwappach, B. (2006) *Biol. Chem.* **387,** 1227–1236
27. Czirják, G., Vuity, D., and Enyedi, P. (2008) *J. Biol. Chem.* **283,** 15672–15680
28. Lu, Z., Abe, J., Taunton, J., Lu, Y., Shishido, T., McClain, C., Yan, C., Xu, S. P., Spangenberg, T. M., and Xu, H. (2008) *Circ. Res.* **103,** 269–278
29. Gao, X., Chaturvedi, D., and Patel, T. B. (2010) *J. Biol. Chem.* **285,** 6970–6979